doi:10.2533/chimia.2023.110 Chimia 77 (2023) 110–115

Enabling Direct Photoelectrochemical H_2 Production Using Alternative Oxidation Reactions on WO_3

Nukorn Plainpan[a], Rangsiman Ketkaew[b], Sandra Luber*[b], and Kevin Sivula*[a]

Abstract: The efficient and inexpensive conversion of solar energy into chemical bonds, such as in H_2 *via* the photoelectrochemical splitting of H_2O, is a promising route to produce green industrial feedstocks and renewable fuels, which is a key goal of the NCCR Catalysis. However, the oxidation product of the water splitting reaction, O_2, has little economic or industrial value. Thus, upgrading key chemical species using alternative oxidation reactions is an emerging trend. WO_3 has been identified as a unique photoanode material for this purpose since it performs poorly in the oxygen evolution reaction in H_2O. Herein we highlight a collaboration in the NCCR Catalysis that has gained insights at the atomic level of the WO_3 surface with *ab initio* computational methods that help to explain its unique catalytic activity. These computational efforts give new context to experimental results employing WO_3 photoanodes for the direct photoelectrochemical oxidation of biomass-derived 5-(hydroxymethyl)furfural. While yield for the desired product, 2,5-furandicarboxylic acid is low, insights into the reaction rate constants using kinetic modelling and an electrochemical technique called derivative voltammetry, give indications on how to improve the system.

Keywords: *ab initio* molecular dynamics methods · Catalysis · Electrosynthesis · Solar energy conversion

Nukorn Plainpan obtained his BSc in Chemistry from Chulalongkorn University, Bangkok, Thailand and a MRes in Green Chemistry: Energy and the Environment from Imperial College, London. He is currently a PhD student at EPFL. His research is mainly focused on the development of photoanodes for biomass valorization applications.

Rangsiman Ketkaew completed his Bachelor's and Master's degrees in chemistry at Thammasat University, Thailand. In 2019, he joined New Equilibrium Biosciences, Boston, MA as an AWS cloud and quantum chemistry consultant. In 2020, he started PhD studies in theoretical chemistry at the University of Zurich. His research focuses on *ab initio* molecular dynamics, enhanced sampling, machine learning, and open-source software development.

Sandra Luber studied chemistry at the University of Erlangen-Nuremberg and ETH Zurich, completing a PhD in (relativistic) quantum chemistry and theoretical spectroscopy. After a postdoctoral stay at the University of Basel and Yale University she changed to industry. Then she joined University of Zurich for a habilitation thesis and was appointed Professor there in 2017. Her research group focuses on the development and application of methods derived from quantum mechanics with emphasis on novel methods for spectroscopy, catalysis, and design of functional compounds.

Kevin Sivula studied chemical engineering at the Universities of Minnesota (Twin Cities), and California (Berkeley), before joining EPFL. He was appointed Assistant Professor in 2011 and Associate Professor in 2018. He leads the Laboratory for molecular engineering of optoelectronic nanomaterials.

1. Introduction

The race towards net-zero carbon emissions demands a shift from our reliance on fossil-fuel-based energy sources to renewable ones. Solar energy alone is more than enough to serve all of our energy needs.[1] However, a major challenge in the reliance on solar energy is the intermittency (day/night and seasonal). To address this challenge, a method to store solar energy is needed over various timescales. Hydrogen (H_2) has emerged as an interesting choice for long-term energy storage thanks to its high energy density (120 MJ/kg).[2] H_2 is easily stored for an extended time and can be used in fuel cells for the generation of electricity when needed. It can also be employed as a chemical feedstock for industry. One way to convert solar energy into H_2 is *via* the (photovoltaic-powered) electrochemical water-splitting reaction (Reaction 1). In an electrochemical cell the water splitting reaction consists of two half-cell reactions: the hydrogen evolution reaction (HER, Reaction 2) and the oxygen evolution reaction (OER, Reaction 3). An externally applied potential will drive the HER at the cathode and the OER at the anode with 1.23 V being

*Correspondence: Prof. K. Sivula[a], E-mail: kevin.sivula@epfl.ch; Prof. S. Luber[b], E-mail: sandra.luber@chem.uzh.ch
[a]Institute of chemical sciences and Engineering, Ecole Polytechnique Federale de Lausanne, CH-1015 Lausanne Switzerland; [b]Department of Chemistry, University of Zurich, CH-8057 Zurich, Switzerland

thermodynamically required for the overall water splitting reaction.

$$H_2O \rightarrow H_2 + \frac{1}{2}O_2 \quad (1)$$

$$2H^+ + 2e^- \rightarrow H_2 \quad (2)$$

$$H_2O \rightarrow \frac{1}{2}O_2 + 2H^+ + 2e^- \quad (3)$$

In practice, the potential required to drive this reaction at a reasonable rate is higher than 1.23 V. The additional voltage required is known as an overpotential and is the result of kinetic barriers, electrical resistance, and mass transfer limitations. The higher the overpotential, the higher the loss in efficiency. Thus, it is desirable to minimize the overpotential as much as possible. For the HER and the OER, the latter has higher overpotential (0.3–0.5 V for a current density >10 mA/cm^2) due to the sluggish reaction kinetics associated with the four-electron OER.[3] Furthermore, O_2, which is the product of the OER, has low economic value since it is readily available from the air. Therefore, many researchers have sought to replace the OER with other oxidation reactions that have faster kinetics, lower thermodynamic potential barriers, and potentially give products with higher economic value.[4–6] One challenge in this regard is the selectivity for the desired alternative reaction over the OER, and this can potentially be addressed using a related technology: photoelectrochemical cells.

Indeed, in addition to the water-splitting electrochemical cell, another way to directly capture and store solar energy as H_2 is by using a photoelectrochemical (PEC) cell. PEC cells utilize a photocathode and a photoanode in tandem to drive the water splitting reaction directly from the sun without external electrical bias.[7] Tungsten trioxide (WO_3) has been shown to possess certain unique properties for use as a photoanode material. This n-type binary oxide is non-toxic and inexpensive which gives this material the potential to be used on large scale. WO_3 also shows great stability in acidic media, a rare behavior for a binary metal oxide semiconductor. While WO_3 has a relatively large bandgap of 2.7–2.8 eV,[8,9] which limits the solar light harvesting WO_3 to harvest only a small part of the solar spectrum, it has been found to have slow kinetics toward the OER, producing peroxide species instead.[10] The oxidation of anions in the electrolyte, such as Cl^- and SO_4^{2-}, have also been reported.[11] These poor kinetics for the OER are normally regarded as a drawback for this material as a photoanode. In contrast they make this material particularly interesting for performing alternative oxidation reactions. Thus a few research groups have recently been investigating the prospect to use a WO_3 photoanode to generate H_2 *via* the PEC oxidation of various substrates and the subsequent reduction of aqueous protons into H_2, as shown schematically in Fig. 1. However, a collaboration between experimental groups and computational groups is needed to better elucidate the properties of this unique material. In this mini review, the recent advances in the use of WO_3 as photoanode material for performing an alternative oxidation reaction will be discussed and how these advances can be complimented by a computational understanding of the unique reactivity of the WO_3 surface will be explored.

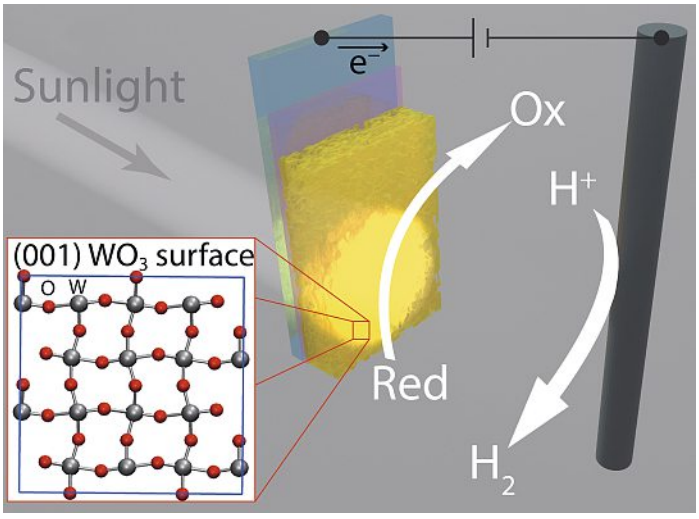

Fig. 1. Schematic of a photoelectrochemical cell with a WO_3 photoanode, immersed in acidic electrolyte, performing a photo-oxidation reaction under illumination while the HER proceeds on the cathode. The inset shows the atomic configuration of the WO_3 (110) surface.

2. Computational Efforts to Understand Catalytic Activity of WO_3 Photoanodes

2.1 *Understanding OER Catalysis at the Atomic Level with ab initio Methods*

Computer simulations can complement experiments, provide indispensable understanding of, and contribute to the determination of reaction mechanisms of catalytic reactions and shed light on the identification and understanding of chemical properties, the role of controlling factors such as experimental conditions, and thermodynamic quantities of the WO_3 metal oxide surface.[12,13] In this section, we discuss recent computational studies on the performance of WO_3 surfaces for the OER and other oxidation reactions. Methods derived from quantum mechanics have been proven to provide a promising avenue for understanding the catalytic activity of metal oxide surfaces at an atomistic level,[14,15] such as the role of oxygen defects causing the formation of oxygen vacancies on the (001) surface of monoclinic WO_3.[16] Besides static calculations, in-depth insight can be obtained by means of so-called *ab initio* molecular dynamics (AIMD), usually based on density functional theory (DFT), which has been used, for example, to treat the dynamics of bulk hexagonal WO_3 in different space groups (P6/*mmm*, P6$_3$/*mcm*, and P6$_3$/*cm*) for investigating electronic and physical properties,[17] and to study the driving force of the catalytic activity regarding the 2-electron water oxidation reaction over WO_3 surfaces with (002), (020), and (200) planes.[18]

Previous works reported results that WO_3 is not entirely without its disadvantages; it is not as abundant and relatively more expensive compared to other transition metals.[19,20] Experimental studies have concluded that WO_3 shows drawbacks compared to other metal oxides in OER catalysis, and computational studies have also supported those studies.[12,21] For example, it is often found that the surface can be oxidized back to WO_3 from other WO_{3-x} surfaces (where x is the fractional value ranging from 0 to 1.5) when exposed to heat and air, reducing its performance for oxidation processes and leading to a low reaction turnover frequency.[22] Several studies have been conducted with the aim to calculate the overpotential of the OER on WO_3 surfaces in various geometries, including different surface orientations, the impact of doping elements on the surface, and oxygen vacancies.[12,23–25] All of these studies have concluded that under typical conditions the OER on WO_3 requires high overpotential, confirming the experimentally observed high overpotential, which can be attributed – according to theoretical evidence – to the slow kinetics of the OER.

2.2 *An Important Role of Hydrophobicity in the Catalytic Performance of WO_3*

A previous study by some of the authors using the sophisticated AIMD technique has revealed that the WO_3 surface is hydrophobic, showing weak interaction between water bulk and the surface, as shown schematically in Figs 2a and 2c, and which can be quantified by means of the radial distribution function between oxygen atoms of water molecules and tungsten atoms of the (001) surface (see Fig. 2b).[13] In addition to that, we recently found by

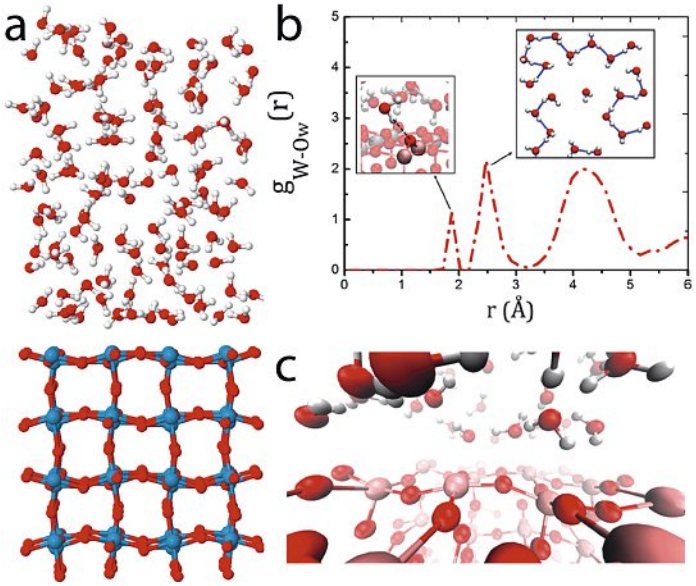

Fig. 2. a) Front-view visualization of WO_3-liquid water interface simulated using DFT-MD simulation (W atoms are blue), b) Radial distribution function between oxygen atoms of water molecules and tungsten atoms at the surface,[13] and c) Enlarged visualization of the vacancy between water molecules and the surface (W atoms are pink). Figures reproduced from ref. [13], copyright 2022, the authors.

AIMD simulations with enhanced sampling techniques that the low catalytic activity of WO_3 for oxygen formation is due to the high barrier for the oxygen–oxygen bond formation (R. Ketkaew, F. Creazzo, K. Sivula, S. Luber, *in preparation*), which leads to a high overpotential, as compared to the benchmark (metal) TiO_2 and RuO_2 systems.[8,26–29] Moreover, the effect of properties of the surface electrode such as the overpotential can relate to the surface hydrophobicity.[30] The computational study by Kishore *et al.*, in which static DFT calculations were used to calculate the OER overpotential of the WO_3 surface with oxygen vacancies, showed that the calculated overpotential mirrors the experimental value, confirming the overpotential regardless of the three surface orientations: (200), (002) and (020).[12]

2.3 *Self-degrading Limitation of the Surface and Catalytic OER*

WO_3 is predicted to be thermodynamically stable when used as a photoanode for the OER due to its anodic decomposition potential which is about 1.1 V more positive than the potential of OER.[20] However, it has been observed that WO_3 gradually loses its catalytic performance over time when used in this setup. In addition, this effect is further exacerbated at higher pH values.[31] Previous works have attributed the degradation of the WO_3 surface to the following reasons:

1. WO_3 is considered an Arrhenius acid, which reduces the stability of the WO_3 surface in basic solutions as the WO_3 has the potential to undergo acid-base reactions with OH^- in solution.[32–34]
2. During the course of (photo)electrochemical OER, WO_3 is known to produce and accumulate (radical) peroxo-species on its surface, followed by the acceleration of its degradation.[10,35]

The decrease in the stability and Faradaic efficiency for OER on WO_3 with increasing pH of the solution is, according to previous computational studies,[21] caused by these two effects.[34,36] Moreover, Ping and Galli investigated computationally orthorhombic WO_3 which is stable at high temperature and found that the orthorhombic crystal system can improve the carrier mobilities for both electron and hole channels. The surface is stabilized, and its self-degrading effect was decreased at ambient conditions resulting in improved properties of WO_3 as a photoanode material.[37]

2.4 *An Important Role of Hydrophobicity in the Catalytic Performance of WO_3*

Although WO_3 shows low activity and high overpotential for the OER,[19] the WO_3 surface has been actively investigated for various catalytic applications, such as alternative oxidation reactions, particularly for reactions that produce valuable oxidation products at stable current densities. Examples include the formation of oxidizing agents like persulfate and sodium hypochlorite,[38] the oxidation of chloride anion to chlorine or hypochlorite,[39] and the oxidation of organic compounds such as 5-(hydroxymethyl) furfural (HMF) to 2,5-furandicarboxylic acid (FDCA)[40–44] due to the fast kinetics of the multi-electron oxidation.[31,45,46] In addition, a DFT study found that it is necessary to increase the energy of the valence band of WO_3 and its band gap to improve the electronic properties of WO_3 surfaces to facilitate those alternative oxidation reactions, as well as to bring it closer to the potential that satisfies water oxidation.[21,47] Therefore, the introduction of alternative oxidation reactions *via* radical species is plausible and may provide an effective avenue to improve and/or design new WO_3 surfaces with high activity.[48] Finally, from theoretical and computational points of view, simulation techniques, particularly AIMD, can serve as a fundamental basis to help the experimental community to investigate the mechanisms of promising alternative oxidation reactions on an atomistic level in great detail.

3. Brief Overview of Alternative Oxidation Reactions

Given the unique surface properties of WO_3, it is a good candidate to drive an oxidation reaction other than the OER. In the field of alternative oxidation reactions and among many possibilities, certain key reactions have been demonstrated as promising replacements for the OER at the anode. Examples of alternative reactions include glycerol oxidation to formic acid[49,50] glucose oxidation to glucaric acid,[51] benzyl alcohol oxidation to benzoic acid,[52–55] and chloride oxidation to chlorine.[56,57] Of these alternative reactions, the oxidation of 5-(hydroxymethyl)furfural (HMF) has received much attention recently.[40,41,58–62] HMF is a biomass-derived product, derived from lignocellulosic biomass, one of the most abundant biomasses on earth.[14] Thus, HMF can be considered a sustainable substrate to replace water. HMF can undergo an overall 6-electron oxidation to 2,5-furandicarboxylic acid (FDCA) in three sequential 2-electron oxidation steps. First, HMF is oxidized to either 2,5-furandicarboxaldehyde (DFF) or 5-hydroxymethyl-2-furan-carboxylic acid (HMFCA). These two intermediates then undergo oxidation into 5-formyl-2-furancarboxylic acid (FFCA) before being subsequently oxidized into the final product FDCA.

Yang and co-workers calculated the standard reduction potential (E^o) of the 6-electron oxidation from HMF to FDCA to be at +0.30 V (compared to +1.23 V for the OER). Nevertheless, the E^o of the 2-electron oxidation from FFCA to FDCA, the final step in the oxidation to FDCA, is calculated to be at +0.43 V.[63] Thus the standard oxidation potential of HMF is significantly lower than that of water oxidation, suggesting that the oxidation of HMF is easier thermodynamically. The product from the HMF oxidation, FDCA, also has a higher commercial value than oxygen. One of the main uses of FDCA is for the production of polyethylene furanoate (PEF). PEF shares many similar properties to polyethylene terephthalate (PET), a plastic that is widely used for food and beverage packaging, showing even lower gas permeability. Indeed, in comparison to PET, the permeability of PEF to O_2 and CO_2 is 11 times and 19 times lower, respectively, a great advantage for a material used for containing food and drinks.[64,65] The Young's modulus of PEF has also been shown to be higher than PET. This can translate into a more resilient final

product.[66] Furthermore, while FDCA is a biomass-derived compound, terephthalic acid, the monomer used to synthesize PET, is made predominantly from petroleum-based compounds.[67] This makes PEF more sustainable than PET. These advantages of PEF have sparked a strong interest to use PEF as a replacement for PET, hence the interest in performing the HMF oxidation reaction instead of the OER in a water splitting photoelectrochemical cell.

4. Direct HMF Oxidation on WO_3 Photoanodes

Despite a number of publications on alternative oxidation reactions using PEC cells,[68–70] the direct photo-driven oxidation of HMF to FDCA has been rarely reported. Cha and co-workers first reported the oxidation of HMF to FDCA on a $BiVO_4$ photoanode.[71] Nevertheless, a redox mediator (2,2,6,6-tetramethylpiperidin-1-yl)oxyl (TEMPO) is required to drive the oxidation of HMF. No noticeable amount of HMF conversion was found in the absence of TEMPO in the electrolyte. The use of a redox mediator adds another complexity to the product purification process. Moreover, any photoanode system performing the HMF oxidation in an aqueous electrolyte potentially has a critical issue: competition of the HMF oxidation with the OER when running the oxidation reaction at a high current density.

As discussed earlier, WO_3 has unique surface properties that make the OER unfavorable, thus suggesting that photo-oxidative selectivity towards direct alternative oxidation reactions should be improved over other systems (*e.g.* $BiVO_4$) that can directly drive the OER. Indeed, the direct oxidation of HMF by WO_3 photoanode was recently demonstrated by EPFL.[36] The activity toward HMF oxidation of WO_3 was first clearly shown by linear sweep voltammetry (LSV) data, as seen in Fig. 3a. Without sunlight, there is no appreciable current density, J, observed versus the reversible hydrogen electrode (RHE) in aqueous conditions (0.1 M sodium phosphate, NaPi, buffer at pH 4). However, when simulated sunlight is incident on the WO_3 photoanode, a photocurrent density is observed that corresponds to the water oxidation reaction. Upon addition of HMF (5 mM), the onset potential of the photocurrent density curve shifts 100 mV cathodically, and the saturated photocurrent density increases by 26% suggesting an ability of WO_3 to directly oxidize HMF. The ability of WO_3 photoanode to oxidize HMF was confirmed by an extended photoelectrolysis experiment. The concentration of HMF drops while the concentration of FDCA and the intermediates (DFF, HMFCA, and FFCA) increase over the course of the reaction, as shown in Figs 3b and 3c, which confirms the ability of the WO_3 photoanode to directly oxidize HMF to FDCA. However, the FDCA yield was found to be very modest at only 0.5%. A kinetic model was developed to improve the understanding of the low FDCA yield. The fit reactions included in the model are shown in Fig. 3d, along with their rate constants. The kinetic model reveals that the rate constants of many modeled competing reactions are larger than the desired reaction (the formation of FDCA). For example, the rate constant for the decomposition of FDCA ($k_{B4} = 72 \times 10^{-3}$ h^{-1}) was also found to be approximately 10 times larger than of its production ($k_3 = 7.3 \times 10^{-3}$ h^{-1}). The faster kinetics of the competing reactions suggest that while the WO_3 photoanode can oxidize HMF to FDCA, this desired pathway is not the most favorable reaction on the surface of WO_3. Therefore, the ability to control the selectivity of the reactions is the key to improving the FDCA yield. To tackle this challenge, a facile technique has been developed to predict the selectivity among competing reactions as a function of the applied potential.[72] The analysis applies the derivative voltammogram technique to the linear sweep voltammogram data and thus is referred to as the ∂J/∂E analysis. In short, applying this analysis affords a deconvolution of the contribution to the photocurrent of multiple competing reactions. This allows one to predict and control the selectivity of the reaction. We demonstrated the use of this analysis to the oxidation of HMF on WO_3 photoanode and found that this technique can be used to predict the selectivity between HMF oxidation and water oxidation.

The analysis predicts that there will be no applied potential which gives an exclusive selectivity toward the oxidation of HMF, and the selectivity will be maximized at 0.66 V vs. RHE (Fig. 4A). The prediction was assessed by comparing to the experimental values at 0.65, 0.85, and 1.20 V vs. RHE (Fig. 4B). Indeed, the selectivity for HMF oxidation does follow the predicted trend. Nevertheless, the prediction is more accurate at the lower applied potential (0.65 V vs. RHE) and starts to deviate from the experimental values at the higher applied potentials (0.85 and 1.20 V vs. RHE). The discrepancy between the predicted and the experi-

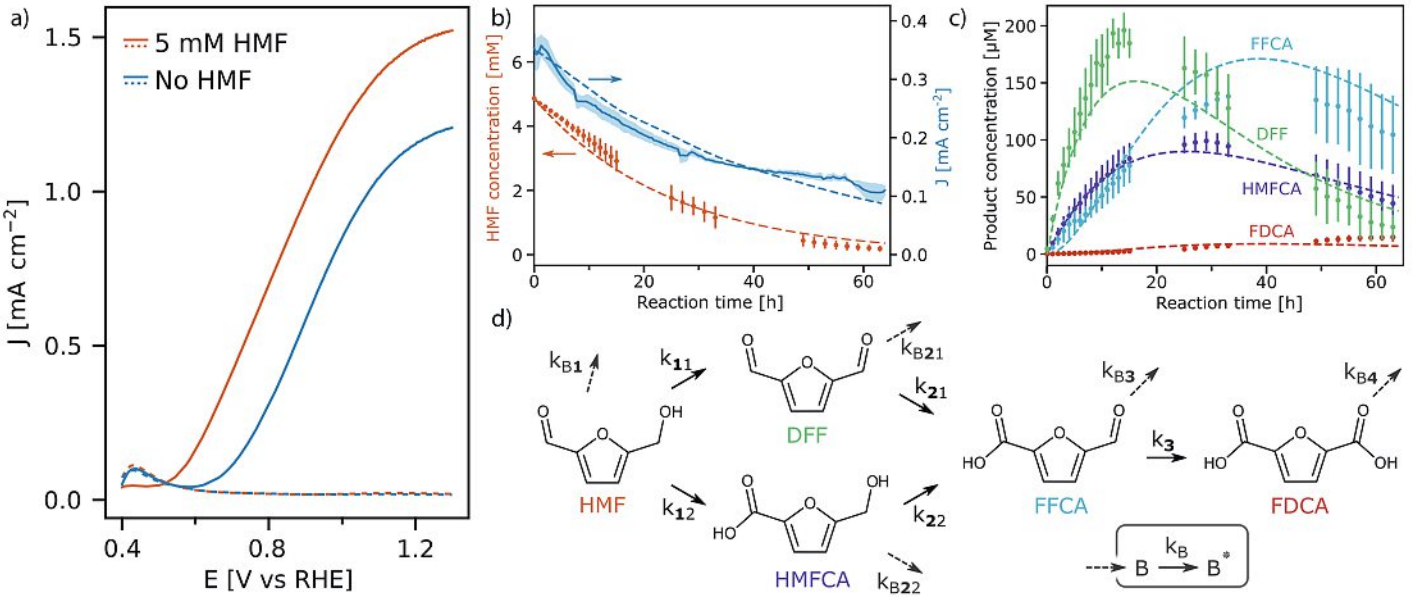

Fig. 3. a) Linear sweep voltammograms of WO_3 photoanode in 0.1 M NaP_i buffer at pH 4 (with and without 5 mM HMF) under illumination (solid) and in the dark (dashed). b) Photocurrent density and the concentration of HMF. c) Concentration of DFF, HMFCA, FFCA and FDCA as the function of reaction time in the photoelectrolysis of HMF over the illuminated surface of WO_3 photoanode (3 suns illumination, pH 4). d) Scheme for the kinetics model for the HMF oxidation reaction with the competing reaction pathways. B and B* represent the byproducts. Adapted from ref. [36], copyright 2021, the authors.

mental values was attributed to kinetics aspects, as the prediction is based purely on thermodynamic rationale. At the higher bias, the kinetics of the reactions (especially for the water oxidation reaction) would have larger effects so that the experimental values deviate from the predicted values. Despite the deviation from the experimental values at the higher applied potential, the analysis can still give an accurate trend of the selectivity as the function of applied potential. Given the fact that this analysis only requires the linear sweep voltammogram, which can be easily obtained with standard electrochemical techniques, this analysis can be a quick tool to estimate the selectivity in the system with competing reactions in PEC cells.

5. Conclusion and Outlook

In this mini-review, we have summarized the recent advances in the use of WO_3 photoanodes in performing alternative oxidation reactions, in particular, HMF oxidation. A number of recent computational studies have revealed that the surface of WO_3 shows a low affinity toward water molecules, leading to poor performance in performing the photo-assisted OER, in accordance with experimental findings. These observations suggest that WO_3 could be an interesting candidate to achieve higher selectivity toward alternative oxidation reactions, when used in a photoelectrochemical cell for H_2 production from aqueous solution. Indeed, WO_3 has been shown to have great potential in performing the alternative oxidation reactions. This oxide has been shown to be the first photoanode material to perform the HMF oxidation to FDCA without any assistance of a redox mediator. The FDCA yield was found to be subtle, which stems from the low reaction selectivity of the HMF oxidation to FDCA reaction as compared to other competing reactions which led to non-desirable side products. To cope with the low selectivity, ∂J/∂E analysis, a method based on a derivative voltammogram, was developed to predict the selectivity of the competing reaction on a photoanode as a function of an applied potential. The analysis requires only the information from standard (photo)electrochemical experiments. This analysis was applied to the oxidation of HMF to FDCA on WO_3 photoanode and the analysis can predict the trend in the selectivity between HMF oxidation and the water oxidation reaction, but the selectivity toward the oxidation to FDCA remains the same regardless of the applied bias.

To advance this concept toward viable real-world application, further understanding of the mechanism for HMF oxidation on the surface of WO_3, aided by the advanced computations techniques described above, will help rationalize the strategy to improve the FDCA yield, enabling the more efficient coupling between HMF oxidation on WO_3 and H_2 production on a photoanode. In addition, the application of tailored co-catalysts to the surface of the WO_3 may further increase the yield of the desired HFM oxidation products and reduce the formation of undesired side products. Finally coupling the WO_3 photoanode with an H_2-producing photocathode in a tandem cell[7] to demonstrate unassisted solar H_2 production with the concurrent photo-electrosynthesis of FDCA, or other oxidatively upgraded chemical product, will be an important step toward validating the system for practical application. In a broader scope, technoeconomic analysis[73] of the envisioned device should be performed to better understand the market advantage of using alternative oxidation reactions instead of the OER in H_2 producing (photo)electrochemical cells, and new materials with unique surface properties like WO_3 while also having a lower semiconductor band-gap to enable greater solar photon harvesting will need to be developed.

Acknowledgements

This publication was created as part of NCCR Catalysis (grant numbers 180544, 1-006445-074), a National Centre of Competence in Research funded by the Swiss National Science Foundation.

Received: December 6, 2022

[1] P. Breeze, in 'Power Generation Technologies', Elsevier, **2019**, pp. 293, https://doi.org/10.1016/B978-0-08-102631-1.00013-4.
[2] S. Chu, in 'AIP Conference Proceedings', *Vol. 1044*, American Institute Of Physics, **2008**, pp. 266, https://doi.org/10.1063/1.2993725.
[3] S. Li, A. Thomas, in 'Advanced Nanomaterials for Electrochemical-Based Energy Conversion and Storage', Elsevier, **2020**, pp. 393, https://doi.org/10.1016/B978-0-12-814558-6.00012-5.
[4] K. Sayama, *ACS Energy Lett.* **2018**, *3*, 1093, https://doi.org/10.1021/acsenergylett.8b00318.
[5] Y. Xu, B. Zhang, *ChemElectroChem* **2019**, *6*, 3214, https://doi.org/10.1002/celc.201900675.
[6] M. T. Bender, X. Yuan, K.-S. Choi, *Nat. Commun.* **2020**, *11*, 4594, https://doi.org/10.1038/s41467-020-18461-1.
[7] M. S. Prévot, K. Sivula, *J. Phys. Chem. C* **2013**, *117*, 17879, https://doi.org/10.1021/jp405291g.
[8] D. Kang, T. W. Kim, S. R. Kubota, A. C. Cardiel, H. G. Cha, K.-S. Choi, *Chem. Rev.* **2015**, *115*, 12839, https://doi.org/10.1021/acs.chemrev.5b00498.
[9] P. González-Borrero, F. Sato, A. Medina, M. L. Baesso, A. C. Bento, G. Baldissera, C. Persson, G. A. Niklasson, C. G. Granqvist, A. Ferreira da Silva, *Appl. Phys. Lett.* **2010**, *96*, 061909, https://doi.org/10.1063/1.3313945.
[10] J. Augustynski, R. Solarska, H. Hagemann, C. Santato, in 'Solar Hydrogen and Nanotechnology', *Vol. 6340*, SPIE, **2006**, pp. 136, https://doi.org/10.1117/12.680667.
[11] J. C. Hill, K.-S. Choi, *J. Phys. Chem. C* **2012**, *116*, 7612, https://doi.org/10.1021/jp209909b.

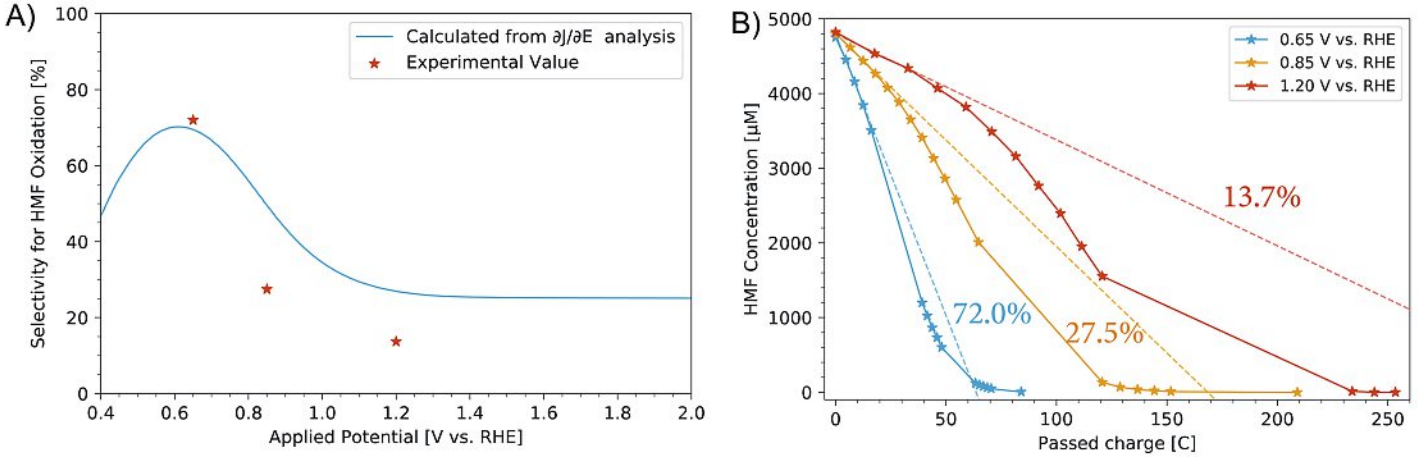

Fig. 4. A) Predicted selectivity and the experimentally determined selectivity between the HMF oxidation and the water oxidation reaction over WO_3 photoanode. B) The concentration of HMF (solid line) with the fitted selectivity from the ∂J/∂E analysis (broken lines) as a function of passed charge at 0.65, 0.85, and 1.20 V vs. RHE. Adapted from ref. [72] with permission from the Royal Society of Chemistry. Copyright The Royal Society of Chemistry 2022.

[12] R. Kishore, X. Cao, X. Zhang, A. Bieberle-Hütter, *Catalysis Today* **2019**, *321–322*, 94, https://doi.org/10.1016/j.cattod.2018.02.030.
[13] F. Creazzo, R. Ketkaew, K. Sivula, S. Luber, *Appl. Surface Sci.* **2022**, *601*, 154203, https://doi.org/10.1016/j.apsusc.2022.154203.
[14] A. M. Abdel-Hamid, J. O. Solbiati, I. K. Cann, in 'Advances in Applied Microbiology', *Vol. 82*, Elsevier, **2013**, pp. 1, https://doi.org/10.1016/b978-0-12-407679-2.00001-6.
[15] S. Americo, E. Pargoletti, R. Soave, F. Cargnoni, M. I. Trioni, G. L. Chiarello, G. Cerrato, G. Cappelletti, *Electrochimica Acta* **2021**, *371*, 137611, https://doi.org/10.1016/j.electacta.2020.137611.
[16] C. Lambert-Mauriat, V. Oison, L. Saadi, K. Aguir, *Surface Sci.* **2012**, *606*, 40, https://doi.org/10.1016/j.susc.2011.08.018.
[17] Y. Lee, T. Lee, A. Soon, *J. Phys. Chem. C* **2018**, *122*, 21644, https://doi.org/10.1021/acs.jpcc.8b05595.
[18] Z. Chen, S. Geng, Y. Wang, Y. Wang, S. Song, *Appl. Catal. B: Environ.* **2022**, *317*, 121756, https://doi.org/10.1016/j.apcatb.2022.121756.
[19] H. Osgood, S. V. Devaguptapu, H. Xu, J. Cho, G. Wu, *Nano Today* **2016**, *11*, 601, https://doi.org/10.1016/j.nantod.2016.09.001.
[20] C. R. Lhermitte, J. G. Verwer, B. M. Bartlett, *J. Mater. Chem. A* **2016**, *4*, 2960, https://doi.org/10.1039/C5TA04747A.
[21] F. Wang, C. Di Valentin, G. Pacchioni, *J. Phys. Chem. C* **2012**, *116*, 8901, https://doi.org/10.1021/jp300867j.
[22] A. Rodríguez-Fernández, L. Bonnet, P. Larrégaray, R. D. Muiño, *Phys. Chem. Chem. Phys.* **2021**, *23*, 7919, https://doi.org/10.1039/D0CP05423B.
[23] V. L. Shaposhnikov, D. B. Migas, V. N. Rodin, V. E. Borisenko, *physica status solidi (b)* **2011**, *248*, 1471, https://doi.org/10.1002/pssb.201046491.
[24] M. D. Bhatt, J. S. Lee, *J. Mater. Chem. A* **2015**, *3*, 10632, https://doi.org/10.1039/C5TA00257E.
[25] H. Ooka, J. Huang, K. S. Exner, *Front. Energy Res.* **2021**, *9*, https://doi.org/10.3389/fenrg.2021.654460.
[26] M. Bele, P. Jovanovič, Ž. Marinko, S. Drev, V. S. Šelih, J. Kovač, M. Gaberšček, G. Koderman Podboršek, G. Dražić, N. Hodnik, A. Kokalj, L. Suhadolnik, *ACS Catal.* **2020**, *10*, 13688, https://doi.org/10.1021/acscatal.0c03688.
[27] S. B. Scott, R. R. Rao, C. Moon, J. E. Sørensen, J. Kibsgaard, Y. Shao-Horn, I. Chorkendorff, *Energy Environ. Sci.* **2022**, *15*, 1977, https://doi.org/10.1039/D1EE03914H.
[28] S. B. Scott, J. E. Sørensen, R. R. Rao, C. Moon, J. Kibsgaard, Y. Shao-Horn, I. Chorkendorff, *Energy Environ. Sci.* **2022**, *15*, 1988, https://doi.org/10.1039/D1EE03915F.
[29] J. C. Hill, K.-S. Choi, *J. Phys. Chem. C* **2012**, *116*, 7612, https://doi.org/10.1021/jp209909b.
[30] J. Bae, I. A. Samek, P. C. Stair, R. Q. Snurr, *Langmuir* **2019**, *35*, 5762, https://doi.org/10.1021/acs.langmuir.9b00577.
[31] C. R. Lhermitte, K. Sivula, *ACS Catal.* **2019**, *9*, 2007, https://doi.org/10.1021/acscatal.8b04565.
[32] J. E. Yourey, B. M. Bartlett, *J. Mater. Chem.* **2011**, *21*, 7651, https://doi.org/10.1039/C1JM11259G.
[33] R. Liu, Y. Lin, L.-Y. Chou, S. W. Sheehan, W. He, F. Zhang, H. J. M. Hou, D. Wang, *Angew. Chem. Int. Ed.* **2011**, *50*, 499, https://doi.org/10.1002/anie.201004801.
[34] R. S. Lillard, G. S. Kanner, D. P. Butt, *J. Electrochem. Soc.* **1998**, *145*, 2718, https://doi.org/10.1149/1.1838704.
[35] J. A. Seabold, K.-S. Choi, *Chem. Mater.* **2011**, *23*, 1105, https://doi.org/10.1021/cm1019469.
[36] C. R. Lhermitte, N. Plainpan, P. Canjura, F. Boudoire, K. Sivula, *RSC Adv.* **2021**, *11*, 198, https://doi.org/10.1039/D0RA09989A.
[37] Y. Ping, G. Galli, *J. Phys. Chem. C* **2014**, *118*, 6019, https://doi.org/10.1021/jp410497f.
[38] H. Ding, J. Hu, *Environ. Res.* **2021**, *201*, 111569, https://doi.org/10.1016/j.envres.2021.111569.
[39] A. G. Breuhaus-Alvarez, Q. Cheek, J. J. Cooper, S. Maldonado, B. M. Bartlett, *J. Phys. Chem. C* **2021**, *125*, 8543, https://doi.org/10.1021/acs.jpcc.0c11282.
[40] Y. Zhao, M. Cai, J. Xian, Y. Sun, G. Li, *J. Mater. Chem. A* **2021**, *9*, 20164, https://doi.org/10.1039/D1TA04981J.
[41] C. Li, Y. Na, *ChemPhotoChem* **2021**, *5*, 502, https://doi.org/10.1002/cptc.202000261.
[42] S. Barwe, J. Weidner, S. Cychy, D. M. Morales, S. Dieckhöfer, D. Hiltrop, J. Masa, M. Muhler, W. Schuhmann, *Angew. Chem. Int. Ed.* **2018**, *57*, 11460, https://doi.org/10.1002/anie.201806298.
[43] N. Zhang, Y. Zou, L. Tao, W. Chen, L. Zhou, Z. Liu, B. Zhou, G. Huang, H. Lin, S. Wang, *Angew. Chem. Int. Ed.* **2019**, *58*, 15895, https://doi.org/10.1002/anie.201908722.
[44] J. Desilvestro, M. Grätzel, *J. Electroanal. Chem. Interfacial Electrochem.* **1987**, *238*, 129, https://doi.org/10.1016/0022-0728(87)85170-7.
[45] C. Debiemme-Chouvy, Y. Hua, F. Hui, J.-L. Duval, H. Cachet, *Electrochimica Acta* **2011**, *56*, 10364, https://doi.org/10.1016/j.electacta.2011.03.025.
[46] F. Dionigi, T. Reier, Z. Pawolek, M. Gliech, P. Strasser, *ChemSusChem* **2016**, *9*, 962, https://doi.org/10.1002/cssc.201501581.
[47] Z. Hajiahmadi, Y. T. Azar, *Surf. Interfaces* **2022**, *28*, 101695, https://doi.org/10.1016/j.surfin.2021.101695.
[48] H. Jin, J. Zhu, W. Chen, Z. Fang, Y. Li, Y. Zhang, X. Huang, K. Ding, L. Ning, W. Chen, *J. Phys. Chem. C* **2012**, *116*, 5067, https://doi.org/10.1021/jp210171f.
[49] X. Han, H. Sheng, C. Yu, T. W. Walker, G. W. Huber, J. Qiu, S. Jin, *ACS Catal.* **2020**, *10*, 6741, https://doi.org/10.1021/acscatal.0c01498.
[50] Y. Chen, A. Lavacchi, H. Miller, M. Bevilacqua, J. Filippi, M. Innocenti, A. Marchionni, W. Oberhauser, L. Wang, F. Vizza, *Nat. Commun.* **2014**, *5*, 1, https://doi.org/10.1038/ncomms5036.
[51] W.-J. Liu, Z. Xu, D. Zhao, X.-Q. Pan, H.-C. Li, X. Hu, Z.-Y. Fan, W.-K. Wang, G.-H. Zhao, S. Jin, G. W. Huber, H.-Q. Yu, *Nat. Commun.* **2020**, *11*, 1, https://doi.org/10.1038/s41467-019-14157-3.
[52] G. Liu, X. Zhang, C. Zhao, Q. Xiong, W. Gong, G. Wang, Y. Zhang, H. Zhang, H. Zhao, *New J. Chem.* **2018**, *42*, 6381, https://doi.org/10.1039/c8nj00446c.
[53] X. Chen, X. Zhong, B. Yuan, S. Li, Y. Gu, Q. Zhang, G. Zhuang, X. Li, S. Deng, J. Wang, *Green Chem.* **2019**, *21*, 578, https://doi.org/10.1039/c8gc03451f.
[54] J. Zheng, X. Chen, X. Zhong, S. Li, T. Liu, G. Zhuang, X. Li, S. Deng, D. Mei, J.-G. Wang, *Adv. Funct. Mater.* **2017**, *27*, 1704169, https://doi.org/10.1002/adfm.201704169.
[55] B. You, X. Liu, X. Liu, Y. Sun, *ACS Catal.* **2017**, *7*, 4564, https://doi.org/10.1021/acscatal.7b00876.
[56] W. Luo, Z. Yang, Z. Li, J. Zhang, J. Liu, Z. Zhao, Z. Wang, S. Yan, T. Yu, Z. Zou, *Energy Environ. Sci.* **2011**, *4*, 4046, https://doi.org/10.1039/c1ee01812d.
[57] S. Iguchi, Y. Miseki, K. Sayama, *Sustain. Energy Fuels* **2018**, *2*, 155, https://doi.org/10.1039/c7se00453b.
[58] D. Zhao, T. Su, Y. Wang, R. S. Varma, C. Len, *Molecular Catal.* **2020**, *495*, 111133, https://doi.org/10.1016/j.mcat.2020.111133.
[59] P. Pal, S. Saravanamurugan, *ChemSusChem* **2019**, *12*, 145, https://doi.org/10.1002/cssc.201801744.
[60] O. Simoska, Z. Rhodes, S. Weliwatte, J. R. Cabrera-Pardo, E. M. Gaffney, K. Lim, S. D. Minteer, *ChemSusChem* **2021**, *14*, 1674, https://doi.org/10.1002/cssc.201801744.
[61] Z. Zhang, K. Deng, *ACS Catal.* **2015**, *5*, 6529, https://doi.org/10.1021/acscatal.5b01491.
[62] F. A. Kucherov, L. V. Romashov, K. I. Galkin, V. P. Ananikov, *ACS Sustain. Chem. Eng.* **2018**, *6*, 8064, https://doi.org/10.1021/acssuschemeng.8b00971.
[63] Y. Yang, T. Mu, *Green Chem.* **2021**, *23*, 4228, https://doi.org/10.1039/d1gc00914a.
[64] S. K. Burgess, O. Karvan, J. Johnson, R. M. Kriegel, W. J. Koros, *Polymer* **2014**, *55*, 4748, https://doi.org/10.1016/j.polymer.2014.07.041.
[65] S. K. Burgess, R. M. Kriegel, W. J. Koros, *Macromolecules* **2015**, *48*, 2184, https://doi.org/10.1021/acs.macromol.5b00333.
[66] K. Loos, R. Zhang, I. Pereira, B. Agostinho, H. Hu, D. Maniar, N. Sbirrazzuoli, A. J. Silvestre, N. Guigo, A. F. Sousa, *Front. Chem.* **2020**, *8*, 585, https://doi.org/10.3389/fchem.2020.00585.
[67] J. J. Pacheco, M. E. Davis, *Proc. Nat. Acad. Sci.* **2014**, *111*, 8363, https://doi.org/10.1073/pnas.1408345111.
[68] Y. He, H. Zhang, Z. Wang, Z. Zheng, P. Wang, Y. Liu, H. Cheng, X. Zhang, Y. Da, B. Huang, *ACS Omega* **2022**, *7*, 12816, https://doi.org/10.1021/acsomega.2c00048.
[69] M. Hambourger, M. Gervaldo, D. Svedruzic, P. W. King, D. Gust, M. Ghirardi, A. L. Moore, T. A. Moore, *J. Am. Chem. Soc.* **2008**, *130*, 2015, https://doi.org/10.1021/ja077691k.
[70] D. Antón-García, E. Edwardes Moore, M. A. Bajada, A. Eisenschmidt, A. R. Oliveira, I. A. Pereira, J. Warnan, E. Reisner, *Nat. Synth.* **2022**, *1*, 77, https://doi.org/10.1038/s44160-021-00003-2.
[71] H. G. Cha, K.-S. Choi, *Nat. Chem.* **2015**, *7*, 328, https://doi.org/10.1038/nchem.2194.
[72] N. Plainpan, F. Boudoire, K. Sivula, *Sustain. Energy Fuels* **2022**, *6*, 3926, https://doi.org/10.1039/d2se00692h.
[73] M. R. Shaner, H. A. Atwater, N. S. Lewis, E. W. McFarland, *Energy Environ. Sci.* **2016**, *9*, 2354, https://doi.org/10.1039/C5EE02573G.

License and Terms

The definitive version of this article is the electronic one that can be found at https://doi.org/10.2533/chimia.2023.110